Biochimica et Biophysica Acta 1797 (2010) 1491–1499

Contents lists available at ScienceDirect

Biochimica et Biophysica Acta

journal homepage: www.elsevier.com/locate/bbabio

Energetics in Photosystem II from *Thermosynechococcus elongatus* with a D1 protein encoded by either the $psbA_1$ or $psbA_3$ gene

Miwa Sugiura [a,*], Yuki Kato [b], Ryouta Takahashi [c], Hiroyuki Suzuki [c], Tadashi Watanabe [b], Takumi Noguchi [c], Fabrice Rappaport [d], Alain Boussac [e]

[a] Cell-Free Science and Technology Research Center, Ehime University, Bunkyo-cho, Matsuyama Ehime, 790-8577, Japan
[b] Institute of Industrial Science, University of Tokyo, 4-6-1 Komaba, Meguro-ku, Tokyo 153-8505, Japan
[c] Institute of Materials Science, University of Tsukuba, Tsukuba, Ibaraki 305-8573, Japan
[d] Institut de Biologie Physico-Chimique, UMR 7141 CNRS and Université Pierre et Marie Curie, 13 rue Pierre et Marie Curie, 75005 Paris, France
[e] iBiTec-S, URA CNRS 2096, CEA Saclay, 91191 Gif-sur-Yvette, France

ARTICLE INFO

Article history:
Received 20 January 2010
Received in revised form 8 March 2010
Accepted 25 March 2010
Available online 31 March 2010

Keywords:
Photosystem II
D1 protein
psbA gene
Electron transfer
Thermosynechococcus elongatus
Pheophytin
Site-directed mutagenesis

ABSTRACT

The main cofactors involved in the function of Photosystem II (PSII) are borne by the D1 and D2 proteins. In some cyanobacteria, the D1 protein is encoded by different *psbA* genes. In *Thermosynechococcus elongatus* the amino acid sequence deduced from the $psbA_3$ gene compared to that deduced from the $psbA_1$ gene points a difference of 21 residues. In this work, PSII isolated from a wild type *T. elongatus* strain expressing PsbA1 or from a strain in which both the $psbA_1$ and $psbA_2$ genes have been deleted were studied by a range of spectroscopies in the absence or the presence of either a urea type herbicide, DCMU, or a phenolic type herbicide, bromoxynil. Spectro-electrochemical measurements show that the redox potential of $Pheo_{D1}$ is increased by 17 mV from −522 mV in PsbA1-PSII to −505 mV in PsbA3-PSII. This increase is about half that found upon the D1-Q130E single site directed mutagenesis in *Synechocystis* PCC 6803. This suggests that the effects of the D1-Q130E substitution are, at least partly, compensated for by some of the additional amino-acid changes associated with the PsbA3 for PsbA1 substitution. The thermoluminescence from the $S_2Q_A^{-\bullet}$ charge recombination and the C≡N vibrational modes of bromoxynil detected in the non-heme iron FTIR difference spectra support two binding sites (or one site with two conformations) for bromoxynil in PsbA3-PSII instead of one in PsbA1-PSII which suggests differences in the Q_B pocket. The temperature dependences of the $S_2Q_A^{-\bullet}$ charge recombination show that the strength of the H-bond to $Pheo_{D1}$ is not the only functionally relevant difference between the PsbA3-PSII and PsbA1-PSII and that the environment of Q_A (and, as a consequence, its redox potential) is modified as well. The electron transfer rate between $P_{680}^{+\bullet}$ and Y_Z is found faster in PsbA3 than in PsbA1 which suggests that the redox potential of the $P_{680}/P_{680}^{+\bullet}$ couple (and hence that of $^1P_{680}^*/P_{680}^{+\bullet}$) is tuned as well when shifting from PsbA1 to PsbA3. In addition to D1-Q130E, the non-conservative amongst the 21 amino acid substitutions, D1-S270A and D1-S153A, are proposed to be involved in some of the observed changes.

1. Introduction

Light-driven water oxidation by the Photosystem II (PSII) enzyme is responsible for the production of O_2 on Earth and is at the origin of the synthesis of most of the biomass. Refined three dimensional X-ray structures from 3.5 to 2.9 Å resolution have been obtained using PSII isolated from the thermophilic cyanobacterium *Thermosynechococcus elongatus* [1–3]. PSII is made up of 17 membrane protein subunits, 3 extrinsic proteins, 35 chlorophyll molecules, 2 pheophytin molecules, 2 hemes, 1 non-heme iron, 2 (+1) quinones, 4 Mn ions, 1 Ca^{2+} ion and at least 1 Cl^- ion, 12 carotenoid molecules and 25 lipids [1–3].

Absorption of a photon by a chlorophyll molecule is followed by the transfer of the exciton to the photochemical trap and the consecutive formation of a radical pair in which the pheophytin molecule, $Pheo_{D1}$, is reduced and the chlorophyll molecule, Chl_{D1}, is oxidized [4–6]. The positive charge is then stabilized on P_{680}, a weakly coupled chlorophyll dimer, see e.g. [7,8] for energetic considerations. The pheophytin anion transfers the electron to a primary quinone electron acceptor, Q_A, which in turn reduces a second quinone, Q_B. $P_{680}^{+\bullet}$ oxidizes a tyrosine residue of the D1 polypeptide, Tyr_Z, which in turn oxidizes the Mn_4Ca-cluster.

Abbreviations: PSII, Photosystem II; Chl, chlorophyll; CP43 and CP47, chlorophyll-binding proteins; DCBQ, 2,6-dichloro-*p*-benzoquinone; PPBQ, phenyl-*p*-benzoquinone; MES, 2-(*N*-morpholino) ethanesulfonic acid; CHES, 2-(Cyclohexylamino)ethanesulfonic acid; Pheo, pheophytin; P_{680}, primary electron donor; Q_A, primary quinone acceptor; Q_B, secondary quinone acceptor; TL, thermoluminescence; OTTLE, optically transparent thin-layer electrode; 43H, *T. elongatus* strain with a His-tag on the C terminus of CP43; WT*, *T. elongatus* strain with a His-tag on the C terminus of CP43 and in which the $psbA_1$ and $psbA_2$ genes are deleted

* Corresponding author. Tel./fax: +81 89 927 9616.
E-mail address: msugiura@chem.sci.ehime-u.ac.jp (M. Sugiura).

0005-2728/$ – see front matter © 2010 Elsevier B.V. All rights reserved.
doi:10.1016/j.bbabio.2010.03.022

The Mn_4Ca-cluster, a device accumulating the four oxidizing equivalents required to split water into dioxygen, is the active site for water oxidation. During the enzyme cycle, the oxidizing side of PSII goes through five sequential redox states, denoted S_n where n varies from 0 to 4 upon the absorption of four photons [9,10]. Upon formation of the S_4 state two molecules of water are rapidly oxidized, the S_0-state is regenerated and O_2 is released.

The main cofactors involved in the function of PSII are borne by D1 and D2 proteins. There are three *psbA* genes encoding the D1 protein in the *T. elongatus* genome [11], corresponding to tlr1843 (*psbA*$_1$), tlr1844 (*psbA*$_2$) and tlr1477 (*psbA*$_3$). The comparison of the amino acid sequence deduced from the *psbA*$_3$ gene to that deduced from the *psbA*$_1$ and *psbA*$_2$ genes points a difference of 21 and 31 residues, respectively. In the nucleotide sequences, 89 nucleotides of *psbA*$_1$ and 170 nucleotides of *psbA*$_2$ differ from the *psbA*$_3$ sequence. Whereas the *psbA*$_1$ and *psbA*$_2$ genes are contiguous in the genome, the initial codon of *psbA*$_2$ being located 312 bp downstream of the terminal codon of *psbA*$_1$, *psbA*$_3$ is located independently and apart from *psbA*$_1$ and *psbA*$_2$.

The presence of several *psbA* genes is a common feature to cyanobacteria [12–15] and these different genes are known to be differentially expressed depending on the environmental conditions [12–23]. In particular, the specific up-regulation of one of these genes under high light conditions points to a role of this response in the overall photo-protection process. Table 1 summarizes the transcription level of the various *psbA* genes found in four cyanobacterial species and a comparison of the amino acid sequences of D1 variants. In *Gloeobacter violaceus* PCC 7421, *Synechocystis* PCC 6803 and *Synechococcus* PCC 7942, UV light and/or high light conditions trigger the expression of a specific *psbA* gene which however encodes a D1 protein identical to the one encoded by the *psbA* gene expressed under normal conditions. In the absence of obvious differences at the protein level, this regulation at the transcription level could be a mean to increase the synthesis of the D1 subunit which is known to be the main target of the light-induced photo-damages. In *Synechococcus* PCC 7942, the *psbAII* gene is up-regulated in high light whereas *psbAI* is down-regulated and D1:2 (products of *psbAII* and *psbAIII*) bears a Glu at position D1–130 in place of a Gln in D1:1 (product of *psbAI*).

Recently, in *T. elongatus*, high light conditions have been shown to induce the expression level of the *psbA*$_3$ gene and to reduce the expression level of the *psbA*$_1$ gene [20,21]. In contrast with the case of the three other cyanobacteria just mentioned above, the D1 sequence from PsbA3 differs significantly from PsbA1 in this organism. This raises the possibility that, in this case, the regulation at the transcription level is not a mere adjustment of the protein synthesis but rather an acclimation at the functional level whereby the functional properties of PSII are adjusted to cope with the increased photon flux.

Amongst the 21 amino acids which differ between PsbA1 and PsbA3, the residue at position 130 has caught much attention. It is a Gln in PsbA1 and a Glu in PsbA3. Raman spectroscopy studies have shown that the 13^1-keto of Pheo is involved in a H-bond [28]. Recent EPR and FTIR studies [29,30] confirmed this point and identified the side-chain of the residue at position 130 of the D1 subunit as the H-bond donor. In addition, the substitution of a glutamine for a glutamate results in a change of the H-bond strength [29,30] and, as the consequence, it modulates the energy level of the $P_{680}^{+\bullet}Pheo_{D1}^{-\bullet}$ radical pair, the free energy change associated with charge separation being larger with Glu than with Gln consistent with the stabilization of the $Pheo_{D1}^{-\bullet}$ anion radical by the stronger H-bond provided by the COOH group than by the $CONH_2$ group [31–34]. A clear and consistent view is thus emerging of the energetic consequences of the D1-Q130E substitution in *Synechocystis* PCC 6803 or *Chlamydomonas reinhardtii*. Importantly, recent thermoluminescence and fluorescence studies of PsbA1 or PsbA3 containing PSII from *T. elongatus* have shown that, although qualitatively consistent with the effect of the D1-Q130E point mutation, the consequences of the PsbA1 for PsbA3 substitution on the kinetics and thermodynamic characteristic of the $S_2Q_A^{-\bullet}$ charge recombination were quantitatively less pronounced [20,35]. This suggests that the physiologically relevant shift from PsbA1 to PsbA3 does not sum-up to the D1-Q130E change and that some (or all) of the 20 additional amino-acid substitutions contribute to determine the overall functional properties of the PsbA3 containing PSII.

The rate of the $S_2Q_A^{\bullet-}$ charge recombination, which has been the main observable used until now to address this issue, is determined by a large variety of thermodynamic and kinetics parameters among which the most important ones are the free energy changes associated with the $P_{680}^{+\bullet}S_1 \leftrightarrow P_{680}S_2$ and $Pheo_{D1}^{-\bullet}Q_A \leftrightarrow Pheo_{D1}Q_A^{-\bullet}$ equilibria and the electron transfer rate of the $P_{680}^{+\bullet}Q_A^{-\bullet} \rightarrow P_{680}Q_A$ charge recombination, see [32,34] for a discussion. To disentangle the interplay of these parameters we have undertaken a more systematic study aimed at characterizing independently the kinetic and thermodynamic characteristics of these different reactions in the PsbA1 and PsbA3 containing PSII from *T. elongatus*.

Altogether, the present data show that the effects of the D1-Q130E substitution are, at least partly, compensated for by some of the additional amino-acid changes associated with the PsbA3 for PsbA1 substitution. We propose that the Q_A pocket and the Q_B environment could be directly or indirectly modified by the D1-S270A substitution and that the P_{680} properties are likely affected by the D1-S153A substitution.

2. Materials and methods

The biological material used was PSII core complexes purified from 1) *T. elongatus* WT* cells, a strain in which both the *psbA*$_1$ and *psbA*$_2$

Table 1
psbA gene expression in four cyanobacterial strains.

Strain	*psbA*	Gene	Level of transcription (mRNA)			Similarity with unprocessed PsbA	Similarity with processed PsbA	D1–130	D1–212	D1–270
			Control conditions	High light conditions	UV light conditions					
T. elongatus[a]	1	tlr1843	+++[b]	<1%	+	100% (360/360)	100% (344/344)	Gln	Cys	Ser
	2	tlr1844	<1%	<1%	<1%	90% (325/360)	91% (313/344)	Glu	Ser	Ala
	3	tlr1477	<1%	+++	++++	94% (339/360)	94% (323/344)	Glu	Ser	Ala
Synechocystis 6803[c,d]	1	slr1181	−	−	?	84% (304/360)	86% (295/344)	Gln	Ala	Ala
	2	slr1311	+++	+++	+	100% (360/360)	100% (344/344)	Gln	Ser	Ser
	3	sll1867	+	+++	+++	100% (360/360)	100% (344/344)	Gln	Ser	Ser
Synechococcus 7942[e,f,g]	1	0424	>80%	+	+	100% (360/360)	100% (344/344)	Gln	Ser	Ser
	2	1389	<20%	++	++	93% (335/360)	93% (321/344)	Glu	Ser	Ser
	3	0893		+	+	93% (335/360)	93% (321/344)	Glu	Ser	Ser
G. violaceus 7421[h]	1	glr2322	+++	++++	+++	100% (360/360)	100% (344/344)	Glu	Ser	Ser
	2	glr0779	+	++	+	100% (360/360)	100% (344/344)	Glu	Ser	Ser
	3	gll3144	≈1%	+++	+	100% (360/360)	100% (344/344)	Glu	Ser	Ser
	4	glr1706	<1%	<1%	<1%	88% (316/360)	88% (303/344)	Glu	Ala	Ser
	5	glr2656	<1%	<1%	<1%	91% (330/360)	93% (322/346)	Glu	Ser	Ser

[a]See [20].
[b]When cells are growing at 60 °C. [c]See [24]. [d]See [27]. [e]See [15]. [f]See [25]. [g]See [26]. [h]See [22].

genes have been deleted and which therefore only expresses *psbA*$_3$ and 2) 43H cell [35,36]. Construction of the His$_6$-tagged strain (the tag on C-terminus of CP43) (43H) and His$_6$-tagged Δ*psbA*$_1$, Δ*psbA*$_2$ strain (WT*) has been described previously [35,36]. PSII purification was done as previously described [35].

Under the growth conditions used here (45–50 °C and ≈60 μE m^{-2} s^{-1}), the 43H cells only expressed PsbA1 as confirmed using the position of the electrochromic band-shift undergone by Pheo$_{D1}$ upon formation of $Q_A^{\bullet-}$ which is at 544.3 nm in PsbA1-PSII and at 547.3 nm in PsbA3-PSII [37] (see also supplementary material).

Absorption changes were measured with a lab-built spectrophotometer [38] where the absorption changes are sampled at discrete times by short flashes. These flashes were provided by a neodymium: yttrium-aluminum garnet (Nd:YAG, 355 nm) pumped optical parametric oscillator, which produces monochromatic flashes (1 nm full-width at half-maximum) with a duration of 5 ns. Excitation was provided by a dye laser (685 nm, 10–15 mJ) pumped by the second harmonic of a Nd:YAG laser. PSII was used at 25 μg of Chl ml^{-1} in 1 M betaine, 15 mM $CaCl_2$, 15 mM $MgCl_2$, and 40 mM MES (pH 6.5). PSII were dark-adapted for 1 h at room temperature (20–22 °C) before the additions of either 0.1 mM Phenyl-*p*-benzoquinone (PPBQ, dissolved in dimethyl sulfoxide) or 0.1 mM DCMU or 0.1 mM bromoxynil (dissolved in ethanol). $P_{680}^{+\bullet}$ reduction was measured in Mn-depleted PSII. Mn-depletion was done as previously described [39] and for the measurements the PSII was resuspended in 0.4 M mannitol, 10 mM $CaCl_2$, 50 mM CHES, pH 9.2. PPBQ was also used at 100 μg ml^{-1}.

Fluorescence changes were measured with the same spectrophotometer using 480 nm as a probe wavelength to excite fluorescence. The probe pulse was filtered out using a combination of KV550 and RG690 and RG695 (Schott) filters. The temperature was controlled with a circulating bath.

Thermoluminescence (TL) glow curves were measured with a lab-built apparatus [40]. PSII were suspended in 1 M betaine, 15 mM $CaCl_2$, 15 mM $MgCl_2$, and 40 mM MES (pH 6.5). The Chl concentration was 0.2 μg of Chl ml^{-1}. PSII were then dark-adapted for 1 h. Just before loading the sample when indicated either 100 μM DCMU or bromoxynil was added to dark-adapted samples containing 15 μg of Chl. The samples were illuminated at 5 °C by using a saturating xenon flash (SL-230 S; Sugawara, Japan) and then rapidly chilled to 77 K with liquid N_2. The frozen samples were then heated at a constant rate of 40 °C min^{-1} and TL emission was detected with a photomultiplier (Hamamatsu, R943-02).

Fe^{2+}/Fe^{3+} FTIR difference spectra were measured as described in [41]. The Mn-depleted PSII samples were suspended in a pH 6.5 MES buffer (10 mM MES, 20 mM sucrose, 5 mM NaCl, and 0.06% dodecyl-β-D-maltoside) in the presence of 10 mM $NaHCO_3$ and 0.25 mM bromoxynil, and concentrated to 9 mg Chl ml^{-1} using Microcon-100 (Amicon). An aliquot (5 μl) of the sample suspension was mixed with 1 μl of 500 mM potassium ferricyanide, and deposited on a CaF_2 plate (25 mm in diameter). The sample was then lightly dried under N_2 gas flow and sandwiched with another CaF_2 plate together with 1 μl of H_2O. One of the CaF_2 plates has a circular groove (14 mm inner diameter; 1 mm width), and the sample cell was sealed with silicone grease laid on the outer part of the groove, where a piece of aluminum foil (~1×1 mm; ~15 μm in thickness) was placed as a spacer. The sample temperature was adjusted to 10 °C by circulating cold water in a copper holder. The sample was stabilized at this temperature in the dark for more than 1 h before starting measurements. Flash-induced FTIR spectra were recorded on a Brucker IFS-66/S spectrophotometer equipped with an MCT detector (D313-L) at 4 cm^{-1} resolution. Flash illumination was performed using a Q-switched Nd:YAG laser (INDI-40-10; 532 nm; ~7 ns fwhm; 10 mJ pulse^{-1} cm^{-2}). Single-beam spectra with 50 scans (25 s accumulation) were recorded before and after single-flash illumination. The measurement was repeated with an interval of 300 s for dark relaxation. The spectra obtained by more than 350 cycles using two samples were averaged to calculate a Fe^{2+}/Fe^{3+} difference spectrum by subtracting the spectrum before illumination from that after illumination.

Spectro-electrochemical measurements were performed as described previously [42]. An air-tight optically transparent thin-layer electrode (OTTLE) cell, served with a Hg-Au mesh working electrode, a Pt black wire counter electrode and an Ag-AgCl (in saturated KCl) reference electrode, was employed for the spectro-electrochemical measurements. The electrode potential is referred to a standard hydrogen electrode (SHE; +199 mV *versus* Ag-AgCl).

In spectro-electrochemical measurements, PSII samples were suspended at a Chl concentration of 0.6 mM, corresponding to ca. 15 μM Pheo$_{D1}$, in a buffer containing 50 mM MES-NaOH (pH 6.5), 0.2 M KCl, 0.2% dodecyl-β-D-maltoside, 1 M betaine, and the following redox mediators: 500 μM anthraquinone (E_m = −225 mV), 500 μM methyl viologen (E_m = −443 mV), and 1,1′-propylene-2,2′-bypyridylium (Triquat, E_m = −556 mV). The PS II sample solution was, after addition of 5 mg ml^{-1} sodium dithionite, transferred to the spectro-electrochemical cell filled with Ar.

Time courses of absorbance change due to photoreduction of Pheo$_{D1}$ were measured using a dual-wavelength spectrophotometer Model V670 (JASCO, Japan) modified for lateral illumination as previously described [42]. Photoreduction of Pheo$_{D1}$ was induced by red actinic light at an intensity of 40 μE m^{-2} s^{-1} from a 500 W Xe lamp (Ushio UXL 500 D-O) with a Toshiba R-65 filter, and the photomultiplier inlet port was protected from the actinic light by two plates of Corning 4-96 filter. The electrode potential was controlled with a potentiostat Model 2020 (Toho Technical Research, Japan). The photoreduction at a series of electrode potentials was performed after at least 40 min after each potential step. The potential step was started first to a negative (reductive) direction, and then to a positive (oxidative) direction.

3. Results

We first focused on the redox properties of Pheo$_{D1}$. The recent development of an electrochemical cell which circumvents the experimental difficulties inherent to titration of strongly reducing species [42] allowed us to compare the redox potential of Pheo$_{D1}$ in PSII obtained from the 43H strain (PsbA1 with D1-Q130, thereafter named PsbA1-PSII) or WT* strain (PsbA3 with D1-E130 thereafter

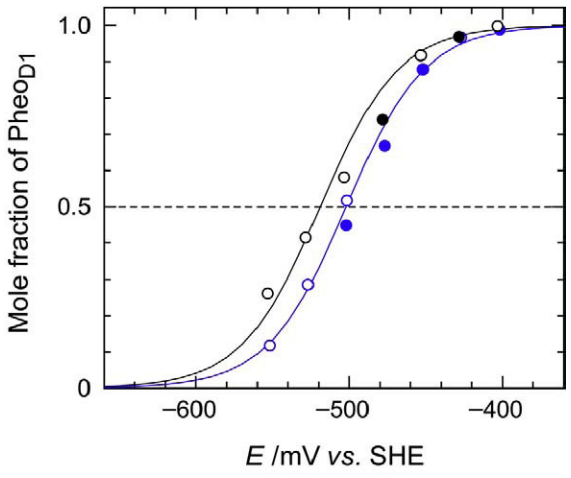

Fig. 1. Nernstian plots for the redox reaction of Pheo$_{D1}$ in PsbA1-PSII (black symbols) and in PsbA3-PSII (blue symbols) based on the ΔA_{450} values at a series of electrode potentials: The data for PsbA1-PSII were based on Fig. S3A, and the data for PsbA3-PSII were cited from the previous measurement [42]. The open and closed symbols were obtained after reductive and oxidative potential steps, respectively. The curves correspond to a one-electron redox process with E_m = −519 mV for PsbA1-PSII and E_m = −502 mV for PsbA3-PSII. Note that these are typical outcome; three independent measurements for PsbA1-PSII yielded a value of −522 ± 3 mV, and −505 ± 6 mV was obtained previously from the four measurements for PsbA3-PSII [42].

named PsbA3-PSII). Fig. 1 shows a typical outcome from spectro-electrochemistry for the redox reaction of $Pheo_{D1}$ in PsbA1-PSII (black) and PsbA3-PS II (blue) (see supplementary material, Fig. S3, for the spectro-electrochemical outcome from PsbA1-PSII; see also [42] for the outcome from PsbA3-PSII). It is shown that the redox potential value of $Pheo_{D1}$ in PsbA1-PSII is ≈17 mV more negative than that in PsbA3-PSII. Three independent measurements for PsbA1-PSII yielded a value of -522 ± 3 and -505 ± 6 mV in PsbA3-PSII after four independent measurements [42]. This shift is qualitatively consistent with the expected strengthening of the H-bond upon the D1-Q130E change, yet it is about half the estimate of 33–38 mV derived from the analysis of the charge separation kinetics or of thermoluminescence measurements in a PSII variant from *Synechocystis* PCC 6803 bearing a Glu in place of the Gln at position D1–130 [31–34].

It is known that, in PSII, the $P_{680}^{+\bullet}Q_A^-$ charge recombination involves either the direct electron transfer between $P_{680}^{+\bullet}$ and $Q_A^{-\bullet}$ (direct pathway) or the thermally activated repopulation of the $P_{680}^{+\bullet}Pheo_{D1}^{-\bullet}$ radical pair (indirect pathway) or the repopulation of the excited state P_{680}^{*} (radiative pathway) [31–34,43]. The yield of the indirect pathways is expected to be significantly affected by a change in the energy gap ΔG_{ind} between $P_{680}^{+\bullet}Pheo_{D1}^{-\bullet}$ and $S_2Q_A^{-\bullet}$ and that of the radiative pathway by a change in the free energy difference ΔG_{cs} between $P_{680}^{+\bullet}Pheo_{D1}^{-\bullet}$ and P_{680}^{*}. Consequently, the difference in the redox potential of the $Pheo_{D1}^{-\bullet}/Pheo_{D1}$ couple in PsbA1-PSII and PsbA3-PSII is expected to translate into changes in the relative yields of these two pathways, unless these different potentials are compensated for, so that the respective free energy differences are kept unchanged. At this stage, it is worth pointing out that the free energy change between P_{680}^{*} and $P_{680}^{+\bullet}Pheo_{D1}^{-\bullet}$ or between $P_{680}^{+\bullet}Pheo_{D1}^{-\bullet}$ and $S_2Q_A^{-\bullet}$ cannot be directly inferred from the difference between the midpoint potentials of the electron donor and acceptor since it includes an additional energetic term corresponding to the electrostatic interaction between the two partners in the radical pair, see [8,42,44] for a discussion. In addition, $Pheo_{D1}$ being a stronger reducing species than Q_A, its redox changes during the electrochemical titration occur in the presence of the reduced form of Q_A and, provided Q_A is in the semiquinone state, this may shift the midpoint potential of $Pheo_{D1}$ with respect to its operating potential as an electron acceptor from P_{680}^{*} or an electron donor to the oxidized form of Q_A. Although these considerations apply when depicting the absolute energy landscape of a reaction center, they will only apply in the present comparative study if the different PsbA forms give rises to different electrostatic interaction. As far as the interaction between $Pheo_{D1}$ and Q_A is concerned this is unlikely since the electrochromic bandshift undergone by $Pheo_{D1}$ upon reduction of Q_A, and thus the electrostatic interaction which triggers it, is of similar magnitude in both PsbA forms (see Fig. S1).

Thermoluminescence is well suited to simultaneously probe both ΔH_{cs} and ΔH_{ind}. As discussed in [45], a change in ΔH_{cs} is expected to affect the intensity of the thermoluminescence band and a change in ΔH_{ind} should translate into a shift of the peak temperature. Fig. 2A shows the TL glow curves arising from the $S_2Q_A^{-\bullet}$ charge recombination in PsbA1-PSII (black trace) and in PsbA3-PSII (blue trace) in the presence of DCMU as an inhibitor of the reoxidation of $Q_A^{-\bullet}$ by Q_B. The peak temperature T_m was similar in the two PSII samples, in agreement with a previous study [35] and the intensity was almost twice larger in the PsbA3-PSII case whereas no significant difference was reported in this respect in [35]. Addressing a similar issue albeit with a different strategy (since the ratio of the PsbA3-PSII to PsbA1-PSII was tuned by changing the light intensity during the *T. elongatus* cells growth), Kos et al. [20] found that the T_m and intensity of the TL curve were respectively down-shifted (by ≈6 °C) and decreased in PsbA3-PSII when compared to PsbA1-PSII as expected if the increased in the redox potential of $Pheo_{D1}^{-\bullet}/Pheo_{D1}$ couple would translate into a smaller ΔH_{ind} and a larger ΔH_{cs}. Confronted to these apparent discrepancies we resorted to an alternative approach to assess the possible changes in ΔG_{ind} occurring when substituting PsbA3 for PsbA1.

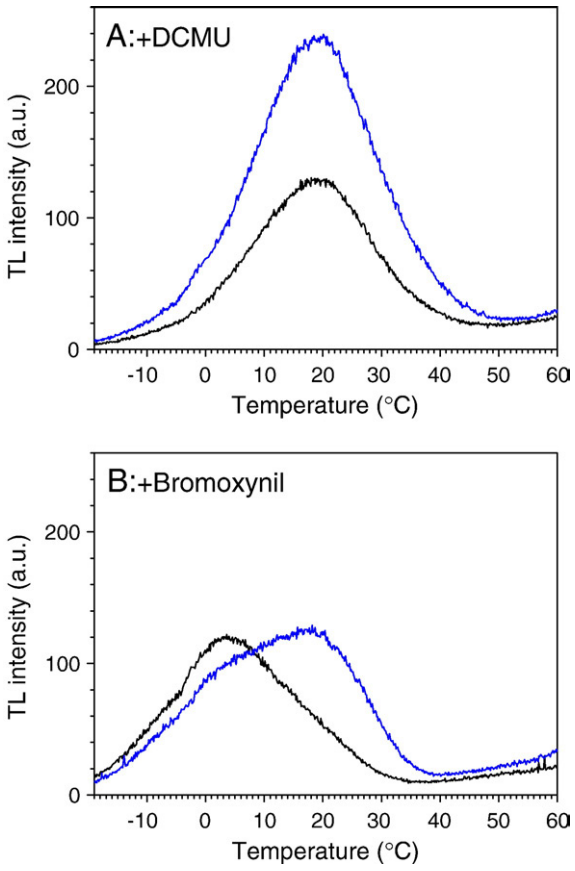

Fig. 2. Thermoluminescence glow curves from $S_2Q_A^{-\bullet}$ charge recombination in the presence of either DCMU (Panel A) or bromoxynil (Panel B) in PsbA1-PSII (black traces) and in PsbA3-PSII (blue traces).

The decay of the $S_2Q_A^{-\bullet}$ state can be followed by measuring the transient changes of the prompt fluorescence yield. These are shown in Fig. 3A, in the presence of DCMU, at 45 °C (solid symbols) and 5 °C (open symbols) for the PsbA3-PSII (blue) and for the PsbA1-PSII (black) samples. At 5 °C, the lifetime of the $S_2Q_A^{-\bullet}$ state was similar or only very slightly longer in PsbA3-PSII than in PsbA1-PSII samples. At 45 °C, the lifetime of the $S_2Q_A^{-\bullet}$ state was similar or only very slightly shorter in PsbA3-PSII than in PsbA1-PSII samples. This suggests that in PsbA3-PSII the free energy difference between $S_2Q_A^{-\bullet}$ and $P_{680}^{+\bullet}Pheo_{D1}^{-\bullet}$ is in fact almost similar (or slightly larger) to that in PsbA1-PSII. This result is in agreement with the TL data presented here and at odds with the conclusion of Kos et al. [20] and with the expectation one could have drawn from the less negative redox potential of the $Pheo_{D1}^{-\bullet}/Pheo_{D1}$ couple. Thus another redox active cofactor rather than $Pheo_{D1}$ most likely undergoes a shift of its redox potential keeping ΔG_{ind} hardly modified despite the 17 meV change in redox potential of the $Pheo_{D1}^{-\bullet}/Pheo_{D1}$ couple. To further characterize the different energy landscape we first scrutinized the environment of Q_A.

Two different classes of compounds are known to inhibit the reoxidation of $Q_A^{-\bullet}$ by Q_B: urea derivatives such as DCMU and phenolic herbicides such as bromoxynil. Importantly, both types of compounds have been shown to modulate the redox potential of the $Q_A^{-\bullet}/Q_A$ couple. DCMU increases the redox potential of $Q_A^{-\bullet}/Q_A$ (making it less negative) and, conversely, bromoxynil decreases the redox potential of $Q_A^{-\bullet}/Q_A$ (making it more negative) [46,47], which suggests different interactions between the quinone and the two herbicides. We thus also studied the effect of bromoxynil addition on the decay of the $S_2Q_A^{-\bullet}$ state in the PsbA3-PSII and PsbA1-PSII either by thermoluminescence studies or by following the fluorescence decay associated with the decay of $Q_A^{-\bullet}$.

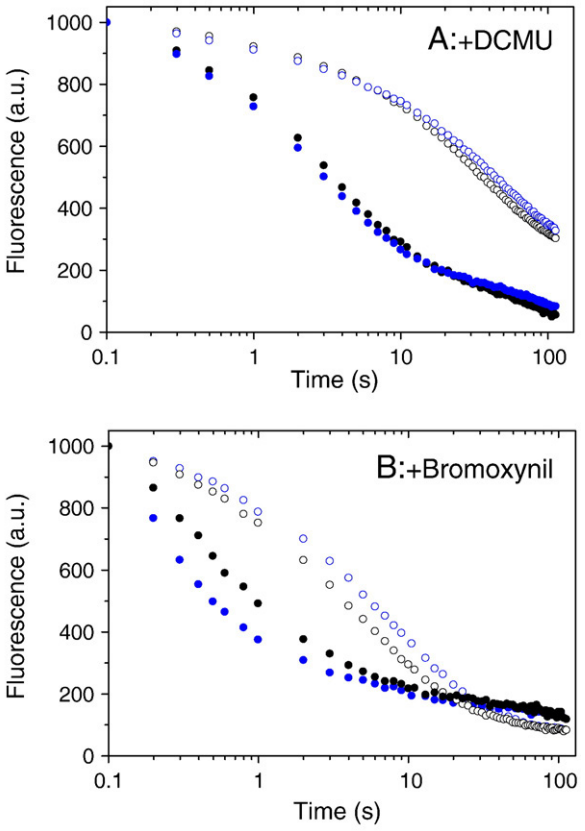

Fig. 3. Fluorescence decay. The dark-adapted samples were illuminated by one saturating flash, then the decay was followed by a train of detecting flashes at the indicated times. The measurements were done in PsbA1-PSII (black symbols) and in PsbA3-PSII (blue symbols) in the presence of either DCMU (Panel A) or bromoxynil (panel B) at 45 °C (full symbols) or 5 °C (open symbols). The traces were normalized to the amplitude of the first point measured at 100 ms after the actinic flash. The samples ([Chl] = 25 μg ml^{-1}) were dark-adapted for 1 h at room temperature before the addition of the herbicide (dissolved in dimethyl sulfoxide) at 100 μM.

Fig. 2B shows the TL curves obtained in the presence of bromoxynil. As previously reported in the case of plant PSII [47], in the PsbA1-PSII the T_m was significantly down-shifted (by ≈20 °C) when compared to the T_m in the presence of DCMU, consistent with the respective redox potential shifts discussed above. In sharp contrast to this, in the PsbA3-PSII case the TL curve showed a major peak with a similar T_m as the one obtained in the presence of DCMU and a minor peak with a T_m similar to the one obtained in the PsbA1-PSII case in the presence of bromoxynil. Before addressing further the origin of this heterogeneity, we will come back to the kinetics and thermodynamics properties in the presence of bromoxynil as characterized by the changes in the fluorescence yield associated with the reoxidation of $Q_A^{-\bullet}$ (Fig. 3). In both the PsbA1-PSII and PsbA3-PSII cases, the decay of the fluorescence yield was significantly faster in the presence of bromoxynil than DCMU. Interestingly, the decay of $Q_A^{-\bullet}$ was significantly faster in the PsbA3-PSII at 45 °C but significantly slower than in the PsbA1-PSII at 5 °C. This suggests a different temperature dependence in the two PSII. We thus studied in more details the decay of $Q_A^{-\bullet}$ as a function of temperature (Fig. 4). Several observations can be made: 1) in the presence of DCMU the Arrhenius plots of the overall charge recombination rate were satisfyingly linear in both the PsbA1-PSII and PsbA3-PSII; 2) in agreement with the trend described above the temperature dependence is slightly steeper in PsbA3 than in PsbA1; 3) in the case of the PsbA1-PSII, the Arrhenius plot was linear as well in the presence of bromoxynil and the slope was steeper in the presence of DCMU than in the presence of bromoxynil, consistent with the respective shifts

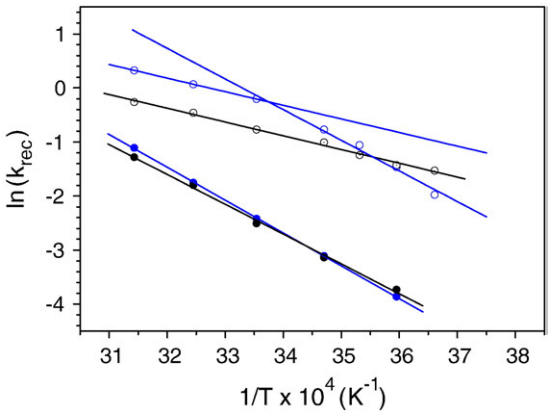

Fig. 4. Arrhenius plot of the fluorescence decays in Fig. 3. Only the global constants (k_{rec} in s^{-1} unit) were estimated. Black symbols, PsbA1-PSII; Blue symbols, PsbA3-PSII; Full symbols, + DCMU: Open symbols, + bromoxynil.

undergone by the redox potential of $Q_A^{-\bullet}/Q_A$ in the presence of these inhibitors; 4) in contrast, in the case of the PsbA3-PSII with bromoxynil, the Arrhenius plot was not linear. The fourth point and the TL data in Fig. 2B strongly suggest a heterogeneity in the process by which $Q_A^{-\bullet}$ decays in PsbA3-PSII in the presence of bromoxynil. Altogether, these data thus point to differences in the interaction between bromoxynil and $Q_A^{-\bullet}/Q_A$ in the PsbA1-PSII and PsbA3-PSII. Formally, the shift undergone by the redox potential of the $Q_A^{-\bullet}/Q_A$ couple upon binding of the herbicide is equivalent to differences in the affinity of the inhibitor for its binding site depending on the redox state of Q_A. Thus, the differences just described should witness at the level of the herbicide binding site.

To investigate this issue we probed the interaction between bromoxynil and the protein moiety by FTIR, using the C≡N frequency mode as a probe. Bromoxynil bears a nitrile group on the phenolic ring, and the C≡N stretching vibration of the nitrile group has a well defined vibration at 2260–2200 cm^{-1} [48], a wavenumber range where proteins and quinone molecules have no absorption bands. In plant PSII, the C≡N stretching frequency of bromoxynil is affected by the redox state of Q_A and bromoxynil has been shown to bind in the phenolate form [49]. Since it has been proposed that bromoxynil interacts with D1-H215 [50,51], a ligand to the non-heme iron, we anticipated a strong sensitivity of the bromoxynil modes to the redox states of the non-heme iron, allowing one to probe the direct environment of bromoxynil *via* the frequencies of its C≡N mode.

Fig. 5 shows the C≡N stretching region of the Fe^{2+}/Fe^{3+} difference spectra of the PsbA1-PSII and PsbA3-PSII in the presence of bromoxynil (The 1800–1000 cm^{-1} region of the spectra are

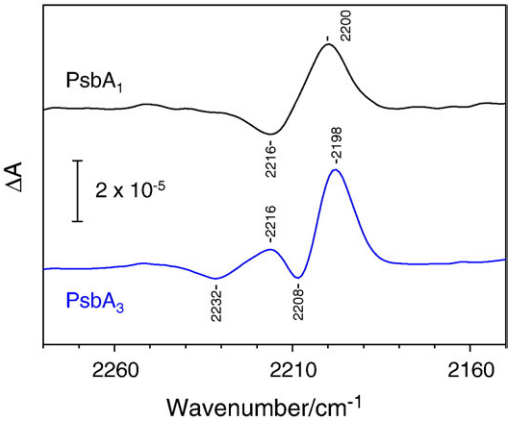

Fig. 5. The C≡N stretching region of the Fe^{2+}/Fe^{3+} FTIR difference spectra of PsbA1-PSII and PsbA3-PSII in the presence of bromoxynil.

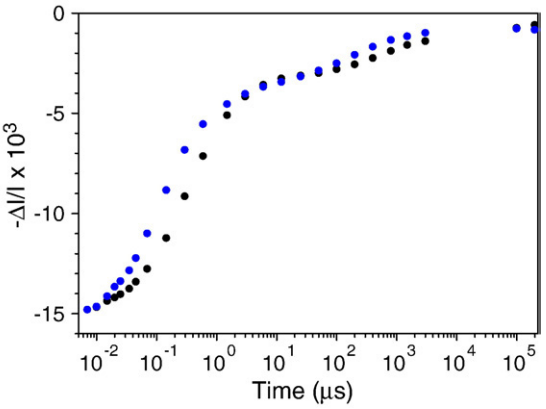

Fig. 6. Kinetics of $P_{680}^{+\bullet}$ reduction in Mn-depleted PSII. The flash-induced absorption changes were measured at 433 nm in PsbA1-PSII (black) and PsbA3-PSII (blue). The dark-adapted samples were illuminated by one saturating flash, then the decay of $P_{680}^{+\bullet}$ was followed by a train of detecting flashes at the indicated times.

presented in Fig. S5). The spectrum exhibits a single differential band at 2200/2216 cm^{-1} with PsbA1-PSII, whereas two differential bands were detected in PsbA3-PSII: the one with the larger amplitude at 2198/2208 cm^{-1} and one with the smaller amplitude at 2216/2232 cm^{-1}. The downshifts of the C≡N frequencies of the nitrile group upon flash illumination shows that as expected the reduction of the non-heme iron from the ferric state Fe^{3+} to the ferrous state Fe^{2+} affects the molecular interaction between the herbicide and its binding pocket. Importantly, these interactions differ between PsbA1-PSII and PsbA3-PSII and, in the latter case, the absorption bands are split in both the reduced and oxidized states, evidencing two distinct conformations for bromoxynil in its site or two different binding sites.

Until now, the comparison of the thermodynamic and kinetic properties of the cofactors of the PsbA1-PSII and PsbA3-PSII has been focused on the electron acceptor side. Modeling of the PsbA3-PSII in the 3.0 Å resolution crystal structure of PSII has pointed however to variations in the vicinity of P_{D1} as well [21] (the D1-S153 residue in PsbA1-PSII is at ≈4.5 Å of P_{D1} and becomes D1-A153 in PsbA3-PSII). Fig. 6 shows that the reduction of $P_{680}^{+\bullet}$ by D1-Y161 (Y_Z) in Mn-depleted PSII was faster in PsbA3-PSII than in PsbA1-PSII, in agreement with our previous report [35]. Recently, the study of the kinetics of $P_{680}^{+\bullet}$ reduction in PsbA1-PSII labeled with 3-fluoro-tyrosine showed that the reduction of $P_{680}^{+\bullet}$ can be described as a sequential process in which the formation of the tyrosinate precedes the electron transfer from the tyrosinate to $P_{680}^{+\bullet}$ [52]. According to this model the reduction rate of $P_{680}^{+\bullet}$ is thus the product between the intrinsic electron transfer rate constant between the tyrosinate and $P_{680}^{+\bullet}$ and the probability for Y_Z to be in the tyrosinate state [52,53]. Importantly, the activation enthalpy of the overall $P_{680}^{+\bullet}$ reduction rate was found little sensitive to a change in the former parameter but significantly modified when changing the latter parameter [53]. We thus measured the temperature dependence of the $P_{680}^{+\bullet}$ reduction rate in Mn-depleted PsbA3-PSII and estimated the activation enthalpy of the fastest component: 125 ± 20 meV (not shown), a figure which is similar to that found in Mn-depleted PsbA1-PSII [52]. The faster reduction rate in PsbA3-PSII thus likely stems from a faster intrinsic electron transfer rate constant between the tyrosinate and $P_{680}^{+\bullet}$. This may reflect a difference in the free energy change associated with the electron transfer from Y_Z to $P_{680}^{+\bullet}$ and thus a different redox potential of either of these two players. As a hint in favor of a change in the redox potential of the $P_{680}^{+\bullet}/P_{680}$ couple we note that the slow component in the reduction of $P_{680}^{+\bullet}$, which develops in the hundreds of microsecond time range and is usually assigned to the charge recombination between $P_{680}^{+\bullet}$ and $Q_A^{-\bullet}$ [54,55] is also faster in PsbA3-PSII than in PsbA1-PSII. However, considering the above discussed evidences that the Q_A pocket also differs between the two types of PSII, this observation cannot be unequivocally interpreted as reflecting a modification of the redox properties of P_{680}.

4. Discussion

In *T. elongatus*, the acclimation to high light intensities induces the expression of the *psbA*$_3$ gene to the detriment of the *psbA*$_1$ gene and the D1 subunit from PsbA3 shows significant differences from that one from the PsbA1. To gain insights into the functional significance of this physiologically relevant acclimation, we have undertaken a comparison between PsbA3-PSII and PsbA1-PSII. As expected from the D1-Q130E substitution, which has been shown to modulate the energy level of the $P_{680}^{+\bullet}Pheo_{D1}^{-\bullet}$ state in site-directed variants of *Synechocystis* PCC 6803 and *C. reinhardtii* [31–34,56], the redox potential of the $Pheo_{D1}^{-\bullet}/Pheo_{D1}$ couple is more negative in PsbA1-PSII (with D1-Q130) than in PsbA3-PSII (with D1-E130). Such a shift has potentially a strong functional significance since, based on the study of site-directed mutants, it translates into a modulation of, on the one hand, the quantum yield of PSII and, on the other hand, of the relative yield of the charge recombination pathway involving the thermally activated formation of $^3[P_{680}^{+\bullet}Pheo_{D1}^{-\bullet}]$ and thus potentially leading to the production of triplet Chl and singlet oxygen, see [47,57] for a discussion. However, the results presented here show that exchanging PsbA1 for PsbA3 does not come down to only tune the redox potential of $Pheo_{D1}^{-\bullet}/Pheo_{D1}$. Indeed, the Q_A pocket also sees its thermodynamic properties changing along with the shift from PsbA1 to PsbA3 and these changes need to be understood before attempting to rationalize their physiological significance.

The slightly enhanced TL intensity observed with PsbA3-PSII with respect to PsbA1-PSII contradicts the expectation one could draw from the shift in redox potential of $Pheo_{D1}^{-\bullet}/Pheo_{D1}$. Indeed, all other things being equal, the less negative redox potential in the PsbA3-PSII translates into a larger free energy difference between $P_{680}^{+\bullet}Pheo_{D1}^{-\bullet}$ and P_{680}^{*} (ΔG_{cs}), which should decrease the relative yield of the radiative charge recombination pathway. Such expectation have been satisfyingly met with site-directed mutant at the position D1–130 as illustrated, for example, by the decreased TL intensity in the D1-Q130E mutant in *Synechocystis* PCC 6803 [34]. At odds with these expectations, PsbA3-PSII exhibited a slightly larger TL intensity than PsbA1-PSII, suggesting that, in contrast to the above discussed expectation, the free energy difference between P_{680}^{*} and $P_{680}^{+\bullet}Pheo_{D1}^{-\bullet}$ in PsbA3-PSII is close to that in PsbA1-PSII (or slightly smaller than in PsbA1-PSII). Consistent with this, we observed no significant differences in the quantum yield of the charge separation, as estimated by the $(F_m - F_0)/F_m$ ratio (0.68 in the two cases, not shown).

The other parameter which is expected to be affected by a modification of the redox potential of $Pheo_{D1}^{-\bullet}/Pheo_{D1}$ is the energy gap between $S_2Q_A^{-\bullet}$ and $P_{680}^{+\bullet}Pheo_{D1}^{-\bullet}$ (ΔG_{ind}) and, as discussed in [45], this should translate into a shifted T_m of the TL curve. Again this expectation was not met since, in the present work, the TL curve of the PsbA3-PSII and PsbA1-PSII had a similar T_m, at variance with the D1-Q130 and D1-E130 variants from *Synechocystis* PCC 6803 [34]. As this will be further discussed below, the similar T_m suggests that the shift of the $Pheo_{D1}^{-\bullet}/Pheo_{D1}$ redox potential is compensated for by a shift of similar amplitude and sign of the $S_2Q_A^{-\bullet}$ and/or $P_{680}^{+\bullet}Q_A^{-\bullet}$ energy level(s). At this stage, we have to note however that the present TL data contradicts those of Kos et al. [20] in which the relative amount of PsbA3 was increased by very high light conditions. The TL curves obtained with strongly illuminated cells enriched in PsbA3-PSII displayed a smaller intensity and a decreased T_m with respect to those obtained with PsbA1-PSII containing cells [20]. Several experimental differences may account for the apparent discrepancies between Kos et al. data and those presented here. First, the heating rate was 20 °C min^{-1} in their case and 40 °C min^{-1} in the present one. Second, here the TL data were

obtained with purified PSII, adapted to darkness for one hour whereas Kos et al. used whole cells with a shorter dark-adaptation. This possibly accounts for variations in the TL intensity since these two procedures likely lead to significantly different fraction of PSII with $Q_B^{-\bullet}$ in the dark. It is well known that addition of DCMU to PSII in the $Q_A/Q_B^{-\bullet}$ state displaces the $Q_A^{-\bullet}Q_B \leftrightarrow Q_AQ_B^{-\bullet}$ equilibrium toward $Q_A^{-\bullet}$DCMU, a state in which no charge separation can be stabilized and therefore which is silent in the TL experiments. In other words, the difference observed in the intensity of the TL curve between PsbA3-PSII and PsbA1-PSII does not necessarily reflect a change in the enthalpy difference between P_{680}^* and $P_{680}^{+\bullet}Pheo_{D1}^{-\bullet}$ and this is all the more so, as the equilibrium $Q_A^{-\bullet}Q_B \leftrightarrow Q_AQ_B^{-\bullet}$ may well differ as well.

An alternative to TL experiment is the estimate of the temperature dependence of the rate of charges recombination in the $S_2Q_A^{-\bullet}$ state. When using DCMU as an inhibitor of the reoxidation of $Q_A^{-\bullet}$ by Q_B, the comparison of the PsbA3-PSII and PsbA1-PSII yielded similar temperature dependence, consistent with the similar T_m obtained here by TL. When using bromoxynil as an inhibitor, the temperature dependence of the decay rate of $Q_A^{-\bullet}$, in the PsbA1-PSII, was less steep than in the presence of DCMU, consistent with the more negative redox potential of $Q_A^{-\bullet}/Q_A$ in the presence of phenolic type herbicides. In the case of the PsbA3-PSII, the Arrhenius plot of the overall decay rate was not linear and could be satisfyingly described by two different slopes. This suggests that, as the temperature is changed, the process underlying the decay of $Q_A^{-\bullet}$ changes. Although this clearly points to heterogeneity, it does not stem from an incomplete occupation of the Q_B pocket by bromoxynil. Indeed we have checked that the concentration used here induced the full inhibition of the PsbA3-PSII turnovers (not shown). In addition, the TL signature of non-inhibited sites would be a band peaking at ≈52 °C corresponding to the $S_2Q_B^{-\bullet}$ TL curve which was not observed. This peculiar temperature dependence and TL profile in the PsbA3-PSII suggests that the interaction between bromoxynil and its binding site (the Q_B pocket) is strongly different. That such is indeed the case is backed-up by the different C≡N modes found for bromoxynil bound to PsbA1-PSII or PsbA3-PSII. In addition, the finding that this mode has two different frequencies in PsbA3-PSII evidences that bromoxynil is found in at least two different conformations in its binding site whereas no such heterogeneity was observed in the PsbA1-PSII. In addition, the FTIR data provide a rationale for the temperature dependence of the decay of $Q_A^{-\bullet}$ and to the heterogeneous TL profile. Indeed, one may consider that the occupation of the two different sites is strongly temperature dependent and that the rate of bromoxynil release from these two sites differs significantly. If the occupation of the "quickly releasing site" increases with temperature, at high temperature $Q_A^{-\bullet}$ would decay through forward electron transfer to Q_B as bromoxynil leaves its site. In this case the rate of decay of $Q_A^{-\bullet}$ would reflect the release of bromoxynil from the "quickly releasing site". At low temperature, where according to this model the "slowly releasing site" would be preferentially occupied, the decay of $Q_A^{-\bullet}$ would reflect the competition between the $S_2Q_A^{-\bullet}$ charge recombination and the equilibrium between the occupancy of the two bromoxynil binding sites. In line with this model, the TL profile was enriched in the high temperature peak as the heating rate was decreased (not shown).

In any case, the TL and temperature dependence data show that the strength of the H-bond to $Pheo_{D1}$ is not the only functionally relevant difference between the PsbA3-PSII and PsbA1-PSII and that the environment of Q_A (and, as a consequence, its redox potential) is modified as well. In addition, we noted earlier that the free energy gap between P_{680}^* and $P_{680}^{+\bullet}Pheo_{D1}^{-\bullet}$ hardly differs in the two PSII despite the different redox potential of $Pheo_{D1}$. This, together with the faster electron transfer rate between $P_{680}^{+\bullet}$ and Y_Z (Fig. 6), suggests that the redox potential of the $P_{680}/P_{680}^{+\bullet}$ (and hence of the $P_{680}^*/P_{680}^{+\bullet}$) is tuned as well when shifting from PsbA1 to PsbA3.

Modeling the PsbA3-PSII into the crystal structure derived from X-ray data collected with PsbA1 containing PSII shows that two variant amino-acids may interact with P_{D1}, D1-S153A interacts with the phytol chain and D1-I184L with the chlorine ring [21] (Fig. S2). As to the acceptor side D1-S270A and D1-C212S interacts, respectively, with the head group of a sulfoquinovosyldiacylglycerol (SQDG) located in the Q_B pocket and with the non-heme iron (Figs. S2 and S4). In plant PsbA, however, the residue at position 212 is a serine (as in the *T. elongatus* PsbA3 case), suggesting that the D1-S270A variant is mostly responsible for the different DCMU/bromoxynil effect between PsbA1 and PsbA3. In addition, Table 1 shows that alanine at position 270 like in PsbA3 is a rare case since *psbA1* in *Synechocystis* PCC 6803 which also contains an alanine is a silent gene. The D1-S270A substitution in PsbA3 may loosen the H-bond with the head group of SQDG and open a second binding pocket for bromoxynil, accounting for the additional C≡N stretching mode. Alternatively, it has been proposed that the oxygen of the phenolate group makes an H-bond with D1-His215, one of the ligand of the non-heme iron [49]. This would change the strength of the hydrogen bond between the CO of Q_A with D2-His214 via the iron-histidine bridge, causing the decrease in the $Q_A^{-\bullet}/Q_A$ redox potential [49]. The heterogeneity in PsbA3-PSII detected in the FTIR and TL experiments could originate from the alteration of the hydrogen-bond strength between bromoxynil and His215 by different conformations in the binding pocket.

As mentioned earlier [35], the oxygen-evolving activity was consistently found higher for PSII with PsbA3 than for PSII with PsbA1 (typically 5000–6000 *versus* 3500–4500 μmol O_2 (mg Chl)$^{-1}h^{-1}$. Nevertheless, until now we found no significant differences in the kinetics of the S_3 to S_0 transition (not shown). This suggests that most of the electron transfer steps which are affected by the PsbA substitution are at the acceptor side level. The present data confirm this hypothesis.

In a recent discussion [57], it was pointed out that the decrease in the energy gap between $Pheo_{D1}^{-\bullet}Q_A$ and $Pheo_{D1}Q_A^{-\bullet}$ in PsbA3-PSII would make the repopulation of the $Pheo_{D1}^{-\bullet}Q_A$ state to the detriment of the direct charge recombination between $P_{680}^{+\bullet}$ and $Q_A^{-\bullet}$ easier in PsbA3-PSII than in PsbA1-PSII when charge recombination occurs from the $Pheo_{D1}Q_A^{-\bullet}$ state. Since the $^3[P_{680}^{+\bullet}Pheo_{D1}^{-\bullet}]$ may be formed from the $^1[P_{680}^{+\bullet}Pheo_{D1}^{-\bullet}]$ state this would imply that finally PsbA3-PSII would be more susceptible to photodamage than PsbA1-PSII. This is a surprising consequence of the D1 substitution since PsbA3 is produced preferentially under high light conditions. To get round this contradiction, the authors in [57] proposed that in fact the $^1[P_{680}^{+\bullet}Pheo_{D1}^{-\bullet}]$ to $P_{680}Pheo_{D1}$ charge recombination occurs in the inverted Marcus region where the rate of the reactions increases when the driving force decreases. This means that the $^1[P_{680}^{+\bullet}Pheo_{D1}^{-\bullet}]$ to $P_{680}Pheo_{D1}$ charge recombination in PsbA3-PSII would occur faster to the detriment of the population of the $^3[P_{680}^{+\bullet}Pheo_{D1}^{-\bullet}]$ state. Although this mechanism could be indeed involved in PsbA3-PSII, this reasoning was only based on the consequences of the D1-Q130E substitution. In the present work it is shown that in addition to the $Pheo_{D1}$ properties, the thermodynamic properties of Q_A, Q_B and P_{680} are also modified in PsbA3-PSII. All these three additional changes are susceptible to favor a more efficient forward electron transfer under high lights conditions like a faster $P_{680}^{+\bullet}$ reduction by Y_Z and a possible higher Q_B availability if the two bromoxynil binding sites suggested above are indicative of two possible Q_B pockets.

Acknowledgments

T.-L. Lai, A.W. Rutherford, N. Ishida, Y. Ohno, H. Ishikita and H. Hayashi are acknowledged for technical help and/or discussions. This study was supported in part by the JSPS and CNRS under the Japan–France Research Cooperative Program, by the EU/Energy project SOLAR-H_2 (contract no. 212508), Grant-in-Aid for scientific research from the Ministry of Education, Science, Sports, Culture and Technology (21612007 for M.S., 21750012 for Y.K., and 21108506,

21370063, and 17GS0314 for T.N.), and Grant-in-Aid for JSPS fellows (204647) to R.T.

Appendix A. Supplementary data

Supplementary data associated with this article can be found, in the online version, at doi:10.1016/j.bbabio.2010.03.022.

References

[1] K.N. Ferreira, T.M. Iverson, K. Maghlaoui, J. Barber, S. Iwata, Architecture of the photosynthetic oxygen-evolving center, Science 303 (2004) 1831–1838.
[2] B. Loll, J. Kern, W. Saenger, A. Zouni, J. Biesiadka, Towards complete cofactor arrangement in the 3.0 Å resolution structure of photosystem II, Nature 438 (2005) 1040–1044.
[3] A. Guskov, J. Kern, A. Gabdulkhakov, M. Broser, A. Zouni, W. Saenger, Cyanobacterial photosystem II at 2.9 Å resolution and the role of quinones, lipids, channels and chloride, Nat. Struct. Mol. Biol. 16 (2009) 334–342.
[4] B.A. Diner, F. Rappaport, Structure, dynamics, and energetics of the primary photochemistry of Photosystem II of oxygenic photosynthesis, Annu. Rev. Plant. Biol. 53 (2002) 551–580.
[5] M.L. Groot, N.P. Pawlowicz, L.J. van Wilderen, J. Breton, I.H. van Stokkum, R. van Grondelle, Initial electron donor and acceptor in isolated Photosystem II reaction centers identified with femtosecond mid-IR spectroscopy, Proc. Natl. Acad. Sci. U. S. A. 102 (2005) 13087–13092.
[6] A.R. Holzwarth, M.G. Muller, M. Reus, M. Nowaczyk, J. Sander, M. Rogner, Kinetics and mechanism of electron transfer in intact photosystem II and in the isolated reaction center: pheophytin is the primary electron acceptor, Proc. Natl. Acad. Sci. U. S. A. 103 (2006) 6895–6900.
[7] F. Rappaport, B.A. Diner, Primary photochemistry and energetics leading to the oxidation of the Mn_4Ca cluster and to the evolution of molecular oxygen in Photosystem II, Coord. Chem. Rev. 252 (2008) 259–272.
[8] G. Renger, A.R. Holzwarth, in: T.J. Wydrzynski, K. Satoh (Eds.), Primary Electron Transfer in Photosystem II: The Light-Driven Water: Plastoquinone Oxidoreductase, Vol. 22, Springer, Dordrecht, 2005, pp. 139–175.
[9] B. Kok, B. Forbush, M. McGloin, Cooperation of charges in photosynthetic O_2 evolution: I. A linear four step mechanism, Photochem. Photobiol. 11 (1970) 457–475.
[10] P. Joliot, B. Kok, Oxygen evolution in photosynthesis, in: Govindjee (Ed.), Bioenergetics of Photosynthesis, Academic Press, New York, 1975, p. 387.
[11] Y. Nakamura, T. Kaneko, S. Sato, M. Ikeuchi, H. Katoh, S. Sasamoto, A. Watanabe, M. Iriguchi, K. Kawashima, T. Kimura, Y. Kishida, C. Kiyokawa, M. Kohara, M. Matsumoto, A. Matsuno, N. Nakazaki, S. Shimpo, M. Sugimoto, C. Takeuchi, M. Yamada, S. Tabata, Complete genome structure of the thermophilic cyanobacterium *Thermosynechococcus elongatus* BP-1, DNA Res. 9 (2002) 123–130.
[12] S.S. Golden, J. Brusslan, R. Haselkorn, Expression of a family of *psbA* genes encoding a photosystem II polypeptide in the cyanobacterium Anacystis nidulans R2, EMBO J. 5 (1986) 2789–2798.
[13] A.K. Clarke, V.M. Hurry, P. Gustafsson, G. Oquist, Two functionally distinct forms of the photosystem-II reaction-center protein D1 in the cyanobacterium *Synechococcus* sp. PCC 7942, Proc. Natl. Acad. Sci. U. S. A. 90 (1993) 11985–11989.
[14] A.K. Clarke, A. Soitamo, P. Gustafsson, G. Oquist, Rapid interchange between two distinct forms of cyanobacterial photosystem-II reaction-center protein-D1 in response to photoinhibition, Proc. Natl. Acad. Sci. U. S. A. 90 (1993) 9973–9979.
[15] S.S. Golden, Light-responsive gene expression in cyanobacteria, J. Bacteriol. 177 (1995) 1651–1654.
[16] D. Campbell, G. Zhou, P. Gustafsson, G. Oquist, A.K. Clarke, Electron transport regulates exchange of two forms of photosystem II D1 protein in the cyanobacterium *Synechococcus*, EMBO J. 14 (1995) 5457–5466.
[17] G. Oquist, D. Campbell, A.K. Clarke, P. Gustafsson, The cyanobacterium *Synechococcus* modulates Photosystem II function in response to excitation stress through D1 exchange, Photosynth. Res. 46 (1995) 151–158.
[18] J. Komenda, H.A. Hassan, B.A. Diner, R.J. Debus, J. Barber, P.J. Nixon, Degradation of the Photosystem II D1 and D2 proteins in different strains of the cyanobacterium *Synechocytis* PCC 6803 varying with respect to the type and level of *psbA* transcript, Plant Mol. Biol. 42 (2000) 635–645.
[19] C.I. Sicora, S.E. Appleton, C.M. Brown, J. Chung, J. Chandler, A.M. Cockshutt, I. Vass, D.A. Campbell, Cyanobacterial psbA families in Anabaena and *Synechocystis* encode trace, constitutive and UVB-induced D1 isoforms, Biochim. Biophys. Acta 1757 (2006) 47–56.
[20] P.B. Kos, Z. Deak, O. Cheregi, I. Vass, Differential regulation of *psbA* and *psbD* gene expression, and the role of the different D1 protein copies in the cyanobacterium *Thermosynechococcus elongatus* BP-1, Biochim. Biophys. Acta 1777 (2008) 74–83.
[21] B. Loll, M. Broser, P.B. Kos, J. Kern, J. Biesiadka, I. Vass, W. Saenger, A. Zouni, Modeling of variant copies of subunit D1 in the structure of photosystem II from *Thermosynechococcus elongatus*, Biol. Chem. 389 (2008) 609–617.
[22] C.I. Sicora, C.M. Brown, O. Cheregi, I. Vass, D.A. Campbell, The *psbA* gene family responds differentially to light and UVB stress in *Gloeobacter violaceus* PCC 7421, a deeply divergent cyanobacterium, Biochim. Biophys. Acta 1777 (2008) 130–139.
[23] P. Mulo, C. Sicora, E.M. Aro, Cyanobacterial *psbA* gene family: optimization of oxygenic photosynthesis, Cell. Mol. Life Sci. 66 (2009) 3697–3710.
[24] A. Mohamed, J. Eriksson, H.D. Osiewacz, C. Jansson, Differential expression of the *psbA* genes in the cyanobacterium *Synechocystis* 6803, Mol. Gen. Genet. 238 (1993) 161–168.
[25] M.R. Schaefer, S.S. Golden, Light availability influences the ratio of two forms of D1 in cyanobacterial thylakoids, J. Biol. Chem. 264 (1989) 7412–7417.
[26] R.D. Kulkarni, S.S. Golden, Adaptation to high light intensity in *Synechococcus* sp. strain PCC 7942: regulation of three *psbA* genes and two forms of the D1 protein, J. Bacteriol. 176 (1994) 959–965.
[27] A. Mohamed, C. Jansson, Influence of light on accumulation of photosynthesis-specific transcripts in the cyanobacterium *Synechocystis* 6803, Plant Mol. Biol. 13 (1989) 693–700.
[28] P. Moënne-Loccoz, B. Robert, M. Lutz, A resonance Raman characterization of the primary electron acceptor in Photosystem II, Biochemistry 28 (1989) 3641–3645.
[29] P. Dorlet, L. Xiong, R.T. Sayre, S. Un, High field EPR study of the pheophytin anion radical in wild type and D1-E130 mutants of photosystem II in Chlamydomonas reinhardtii, J. Biol. Chem. 276 (2001) 22313–22316.
[30] Y. Shibuya, R. Takahashi, T. Okubo, H. Suzuki, M. Sugiura, T. Noguchi, Hydrogen bond interaction of the pheophytin electron acceptor and its radical anion in Photosystem II as revealed by Fourier Transform Infrared Difference Spectroscopy, Biochemistry 49 (2010) 493–501.
[31] S.A.P. Merry, P.J. Nixon, L.M.C. Barter, M.J. Schilstra, G. Porter, J. Barber, J.R. Durrant, D. Klug, Modulation of quantum yield of primary radical pair formation in photosystem II by site directed mutagenesis affecting radical cations and anions, Biochemistry 37 (1998) 17439–17447.
[32] F. Rappaport, M. Guergova-Kuras, P.J. Nixon, B.A. Diner, J. Lavergne, Kinetics and pathways of charge recombination in Photosystem II, Biochemistry 41 (2002) 8518–8527.
[33] A. Cuni, L. Xiong, R.T. Sayre, F. Rappaport, J. Lavergne, Modification of the pheophytin midpoint potential in Photosystem II: modulation of the quantum yield of charge separation and of charge recombination pathways, Phys. Chem. Chem. Phys. 6 (2004) 4825–4831.
[34] K. Cser, I. Vass, Radiative and non-radiative charge recombination pathways in Photosystem II studied by thermoluminescence and chlorophyll fluorescence in the cyanobacterium *Synechocystis* 6803, Biochim. Biophys. Acta 1767 (2007) 233–243.
[35] M. Sugiura, A. Boussac, T. Noguchi, F. Rappaport, Influence of histidine-198 of the D1 subunit on the properties of the primary electron donor, P_{680}, of Photosystem II in *Thermosynechococcus elongatus*, Biochim. Biophys. Acta 1777 (2008) 331–342.
[36] M. Sugiura, Y. Inoue, Highly purified thermo-stable oxygen-evolving photosystem II core complex from the thermophilic cyanobacterium *Synechococcus elongatus* having His-tagged CP43, Plant Cell Physiol. 40 (1999) 1219–1231.
[37] J.L. Hughes, N. Cox, A.W. Rutherford, E. Krausz, T.L. Lai, A. Boussac, M. Sugiura, D1 protein variants in Photosystem II from *Thermosynechococcus elongatus* studied by low temperature optical spectroscopy, Biochim. Biophys. Acta 1797 (2010) 11–19.
[38] D. Beal, F. Rappaport, P. Joliot, A new high-sensitivity 10-ns time-resolution spectrophotometric technique adapted to in vivo analysis of the photosynthetic apparatus, Rev. Sci. Instrum. 70 (1999) 202–207.
[39] S. Un, A. Boussac, M. Sugiura, Characterization of the tyrosine-Z radical and its environment in the spin-coupled $S_2Tyr_Z^{\bullet}$ state of Photosystem II from *Thermosynechococcus elongatus*, Biochemistry 46 (2007) 3138–3150.
[40] T. Noguchi, M. Katoh, Y. Inoue, A new system for detection of thermoluminescence and delayed fluorescence from photosynthetic apparatus with precise temperature control, Spectroscopy 16 (2002) 89–94.
[41] R. Takahashi, A. Boussac, M. Sugiura, T. Noguchi, Structural coupling of a tyrosine side chain with the non-heme iron center in photosystem II as revealed by light-induced Fourier transform infrared difference spectroscopy, Biochemistry 48 (2009) 8994–9001.
[42] Y. Kato, M. Sugiura, A. Oda, T. Watanabe, Spectroelectrochemical determination of the redox potential of pheophytin a, the primary electron acceptor in photosystem II, Proc. Natl. Acad. Sci. U. S. A. 106 (2009) 17365–17370.
[43] H.J. van Gorkom, Electron transfer in photosystem II, Photosynth. Res. 6 (1985) 97–112.
[44] J. Alric, A. Cuni, H. Maki, K.V. Nagashima, A. Verméglio, F. Rappaport, Electrostatic interaction between redox cofactors in photosynthetic reaction centers, J. Biol. Chem. 279 (2004) 47849–47855.
[45] F. Rappaport, J. Lavergne, Thermoluminescence: theory, Photosynth. Res. 101 (2009) 205–216.
[46] A. Krieger, A.W. Rutherford, G.N. Johnson, On the determination of redox midpoint potential of the primary quinone electron acceptor, QA, in photosystem II, Biochim. Biophys. Acta 1229 (1995) 193–201.
[47] A. Krieger-Liszkay, A.W. Rutherford, Influence of herbicide binding on the redox potential of the quinone acceptor of photosystem II: relevance to photodamage and phytotoxicity, Biochemistry 37 (1998) 17339–17344.
[48] G. Socrates, Infrared Characteristic Group Frequencies, John Wiley & Sons, Chichester, U.K., 1994, p. 54.
[49] A. Takano, R. Takahashi, H. Suzuki, T. Noguchi, Herbicide effect on the hydrogen-bonding interaction of the primary quinone electron acceptor QA in photosystem II as studied by Fourier transform infrared spectroscopy, Photosynth. Res. 98 (2008) 159–167.
[50] A. Trebst, The three-dimensional structure of the herbicide binding on the reaction center polypeptides of photosystem II, Z. Naturforsch. 42c (1987) 742–750.
[51] V. Sobolev, M. Edelman, Modeling the quinone-B binding site of the photosystem-II reaction center using notions of complementarity and contact-surface between atoms, Proteins 21 (1995) 214–225.
[52] F. Rappaport, A. Boussac, D.A. Force, J. Peloquin, M. Brynda, M. Sugiura, S. Un, R.D. Britt, B.A. Diner, Probing the coupling between proton and electron transfer in photosystem II core complexes containing a 3-fluorotyrosine, J. Am. Chem. Soc. 131 (2009) 4425–4433.

[53] F. Rappaport, J. Lavergne, Coupling of electron and proton transfer in the photosynthetic water oxidase, Biochim. Biophys. Acta 1503 (2001) 246–259.
[54] G. Renger, C. Wolff, Existence of a high photochemical turnover rate at reaction centers of system-2 in tris-washed chloroplasts, Biochim. Biophys. Acta 423 (1976) 610–614.
[55] J. Haveman, P. Mathis, Flash-induced absorption changes of primary donor of photosystem-ii at 820 nm in chloroplasts inhibited by low ph or tris-treatment, Biochim. Biophys. Acta 440 (1976) 346–355.
[56] L.B. Giorgi, P.J. Nixon, S.A.P. Merry, D.M. Joseph, J.R. Durrant, J.D. Rivas, J. Barber, G. Porter, D.R. Klug, Comparison of primary charge separation in the photosystem II reaction center complex isolated from wild-type and D1–130 mutants of the cyanobacterium Synechocystis PCC 6803, J. Biol. Chem. 271 (1996) 2093–2101.
[57] I. Vass, K. Cser, Janus-faced charge recombinations in photosystem II photoinhibition, Trends Plant Sci. 14 (2009) 200–205.